Stability and flexibility of self-assembled monolayers of thiols consisting of a horizontal large π-system and a vertical spacer

2008 J. Phys.: Condens. Matter 20 315012

(http://iopscience.iop.org/0953-8984/20/31/315012)

J. Phys.: Condens. Matter **20** (2008) 315012 (7pp) doi:10.1088/0953-8984/20/31/315012

Stability and flexibility of self-assembled monolayers of thiols consisting of a horizontal large π-system and a vertical spacer

Rui-Fen Dou[1,2], Xu-Cun Ma[2], Luan Xi[1], Hin Lap Yip[1], King Young Wong[1], Woon Ming Lau[1,3,7], Xiao-Li Fan[1,3,4], Jin-Feng Jia[2], Qi-Kun Xue[2,7], W S Yang[5], Hong Ma[6] and Alex K-Y Jen[6]

[1] Department of Physics and Materials Science and Technology Research Center, The Chinese University of Hong Kong, Shatin, Hong Kong, People's Republic of China
[2] Institute of Physics, Chinese Academy of Sciences, Beijing 100080, People's Republic of China
[3] Surface Science Western, University of Western Ontario, London, ON, N6A 5B7, Canada
[4] School of Materials Science and Engineering, Northwestern Polytechnic University, Xian, People's Republic of China
[5] Department of Physics, Peking University, Beijing 100871, People's Republic of China
[6] Department of Materials Science and Engineering, University of Washington, Seattle, WA 98195, USA

E-mail: llau22@uwo.ca and qkxue@aphy.iphy.ac.cn

Received 18 April 2008, in final form 29 June 2008
Published 17 July 2008
Online at stacks.iop.org/JPhysCM/20/315012

Abstract

Self-assembled monolayers (SAMs) of (4-mercaptophenyl) (10-nitro-9-anthryl) acetylene (MPNAA) on Au(111) are studied with scanning tunneling microscopy (STM). Through careful analysis of the bias-dependent sub-molecular features observed in the high-resolution STM images, important structural details of the MPNAA SAM are disclosed, in addition to its structural character common for the anthracene-based thiol SAMs studied in a recent paper (Dou *et al* 2006 *Langmuir* **22** 3049). With these experimental results, a new model is proposed for the SAM structure to explain, particularly, the molecule–substrate, molecule–molecule and intramolecular interactions, as well as their competitions and compromises in the formation of the SAM structure. Flexibilities and application potentials of the SAMs of thiols based on a long π-system (like that of anthracene or even pentacene) arranged horizontally and a vertical spacer (like the phenyl–acetylene group) are also discussed.

(Some figures in this article are in colour only in the electronic version)

1. Introduction

Thiol-derived self-assembled monolayers (SAMs) on noble metal substrates, especially gold, are of great importance in a variety of applications, and have been widely studied [1–3]. For example, SAMs of large molecules like porphyrin and phthalocyanine thiols have been attracting much attention [4–7]. However, in terms of assembly structures as well as their driving forces, essentially only SAMs of the aliphatic thiols and thiols with an oligophenyl group are relatively well understood, while in such cases each molecule occupies only a small substrate area covering 3 or so gold atoms [1–3]. Although the assembly structures of thiols with a naphthalene, an anthracene, or a similar aromatic group have

[7] Authors to whom any correspondence should be addressed.

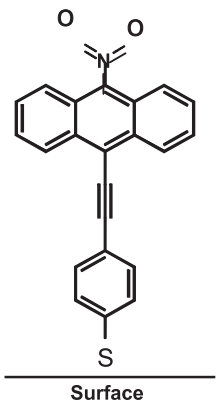

Chart 1. Side view of a MPNAA molecule adsorbed on the gold surface.

been studied, the long axis of the aromatic groups for these reported molecules are parallel to the long axis of the thiols such that the aromatic groups formed the so-called herringbone structure and each molecule still only occupies a substrate area of only 3 or so gold atoms [8].

Recently, thiol SAMs where each molecule occupies a substrate area much larger than 3 gold atoms have been studied [9–11], and plausible models derived from experimental high-resolution scanning tunneling microscopic (STM) images have been proposed for their structures [11]. According to the models, the parallel-displaced π–π stacking interactions, which have long been known to be the dominant force in the stabilization of the double helical structures of DNA and the tertiary structures of proteins [12, 13], could also enable large π-molecules, such as the anthracene-based thiols studied there, to self-assemble into stable and well-ordered structures on gold substrates. Moreover, the SAMs studied there exhibit a prominent common character, that is, each molecule in the SAMs occupies a large substrate area of 7 or more gold atoms [11]. In order to take advantage of this character for future design of specific SAMs, one should understand the role played by the substrate–adsorbate and adsorbate–adsorbate interactions in the SAMs, because it is generally believed that organization of complex, semiflexible organic molecules into SAMs is the result of a delicate interplay between the substrate–adsorbate and adsorbate–adsorbate interactions, as well as the intramolecular interactions in some cases [1–3].

In the present paper, we revisit the SAM of (4-mercaptophenyl) (10-nitro-9-anthryl) acetylene (MPNAA, see chart 1), one of the four anthracene-based thiols studied previously [11], to understand more about the delicate interplay between the involved interactions. MPNAA is chosen because (i) it consists of a tail group, which is important in application; (ii) inclusion of a tail group of nitro results in a molecular dipole moment, a mild but important kind of adsorbate–adsorbate interaction which is quite common in many molecule systems [14]; and (iii) the nitro group on top of the molecule is expected to give rise to some interesting bias-dependent STM features.

2. Experimental details

The MPNAA SAMs were prepared by immersing the Au(111) substrates into a 50 μM dilute ethanol/MPNAA solution at room temperature (RT) for more than 48 h. The details of preparation of the Au(111) substrates and MPNAA SAM samples have been reported previously [11]. The MPNAA samples were then transferred into a UHV chamber for the STM study. Our STM measurements were performed in an OMICRON ultra-high vacuum scanning probe microscopy (UHV-SPM) system with a base pressure of 5×10^{-10} Torr. All STM images shown here were obtained at RT by using the constant current mode and the Pt–Ir tips chemically etched with alternating-current. The tunneling current was set between 10 and 70 pA, and the bias voltage was in the range from -1.7 to $+1.7$ V with the sample grounded. The voltage-dependent STM images were obtained by using carefully prepared stable tips, and their measurements were very reproducible.

3. Results and discussion

In comparison to the STM results reported and discussed in the previous study of MPNAA on Au(111), the present study gives many new details of the MPNAA molecular packing structure. This is evident in the series of occupied-state STM images of the MPNAA SAM which are collected at different STM tip biases and are shown in figure 1. In essence, the STM imaging measurements consistently show that the occupied-state images acquired at a negative sample bias of -1.0 V (figure 1(a)) and -0.6 V (figure 1(b)) are virtually the same. They are also seemingly the same as the empty-state STM images, such as those taken at 0.4 V and reported in our previous study [11]. In these images each molecule is imaged as a single oblong protrusion, and the protrusions are arranged into a two dimensional lattice with the two unit vectors being **a** and **b**. The protrusions are aligned into wavelike rows in the direction of **a**, with the wavelength of four protrusions, which has been explained in our previous study [11] as a consequence of the expected parallel-displaced π–π interactions between adjacent anthryl units. The most enlightening information in the STM imaging results of figure 1 is, however, not this similarity but the variation of STM contrast and the emergence of some fine structures in the same unit cell when the bias is set around -0.4 V (figure 1(c)). Among these changes, the emergence of two small protruding-dot features with a separation of about 3 Å is most intriguing as it decorates each 'molecule' of the unit cell and makes them slightly different from each other. The additional STM imaging information revealed by figure 1(c) inevitably requires a revisit and revision of the molecular models of MPNAA and related aromatic molecules reported earlier [11].

The rich STM imaging features revealed in figure 1(c) fade quickly when the bias is moved away from -0.4 V. For example, figure 1(d) shows the STM image at -0.2 V; the fine structures in figure 1(c) are no longer clear. With the assumption that the image features of figure 1(c) arise from electrons tunneling to the STM tip from the local density of

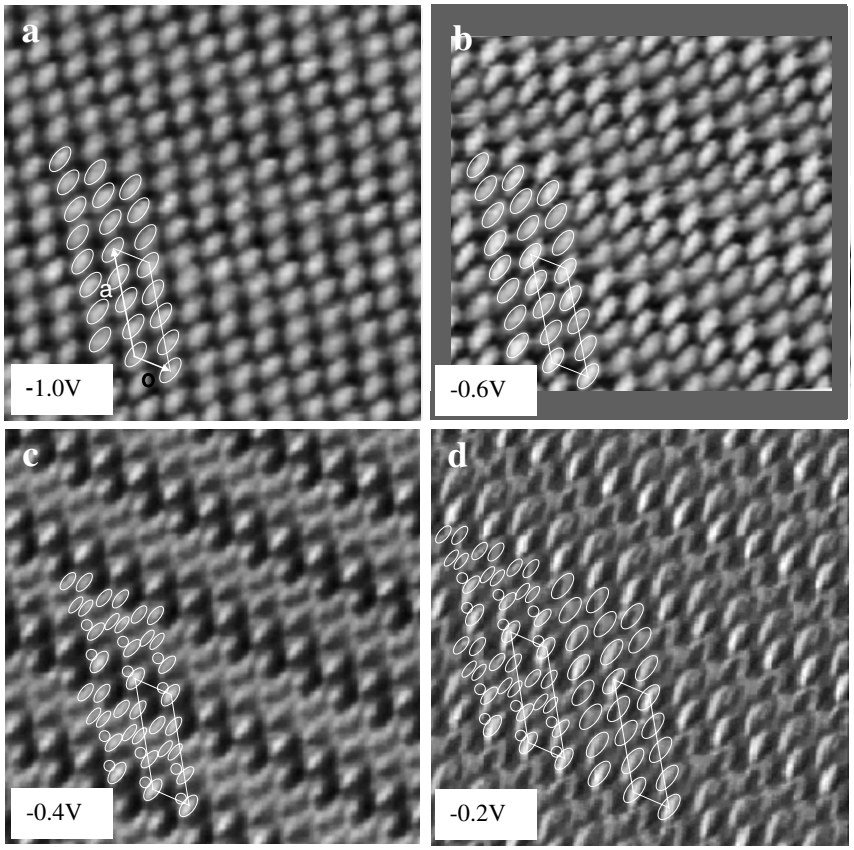

Figure 1. Bias-dependent occupied-state STM images obtained from the MPNAA SAM. The sample-relative-to-tip bias voltages are shown at the lower-left corner of the corresponding images, and the tunneling current is 0.04 nA for these images. The lengths of unit vector *a* and *b* are 28.0 Å and 9.8 Å, respectively, and the angle between the two vectors is 56°. The image sizes for (a), (c), and (d) are 15 × 15 nm^2, while for (b) it is 12 × 11 nm^2.

states (LDOS) of the SAM of MPNAA on gold, the 'band width' of the corresponding LDOS must be quite narrow.

In the interpretation of STM images, one needs to consider the following two key attributes: (a) LDOS of the molecular system being probed, as a function of energy measured from the Fermi level; and (b) the spatial separation between the tip and the LDOS source. Here, the tip is assumed to have a featureless DOS at its Fermi level such that the electronic interactions between the tip and the molecular system being probed can be simplified to: either electrons in the occupied LDOS tunneling to the Fermi level of the tip, or electrons tunneling to the empty LDOS from the Fermi level of the tip. In the context of discussing the effects of the LDOS of the molecular system being probed in the present case of MPNAA on gold, it is also important to focus on the LDOS of MPNAA on gold instead of the molecular states of a 'free' MPNAA molecule. For example, an *ab initio* computation[8] conducted in parallel to the present experimental STM studies indicates that when 2-nitro-anthryl thiol molecules are adsorbed on Au(111), the highest occupied LDOS band is located at around −0.5 eV and the lowest unoccupied LDOS band at 1–2 eV. The LDOS calculation results are summarized in figure 2. In the language of linear combination of atomic orbitals (LCAOs), the LDOS band at −0.5 eV is mainly derived from C $2p_y$, with some small contributions from O $2p_z$ and S $2p_y$ (z is the direction of the C–N bond; y is the normal of the anthryl plane; and x is the direction of the long axis of the anthryl plane). As shown in figure 2, the band intensity rises near the Fermi level and falls down quickly before −1 eV; hence, the bandwidth is quite narrow. For a low tip–sample bias of −0.4 V, the tip is expected to receive electrons from this narrow band. Since the tip is approaching the adsorbed molecule (in a standing-up configuration) from the nitro tail end, it will first encounter the O $2p_z$ components of the LDOS band below the Fermi level before it can sense the C $2p_y$ components of the LDOS band. If it can collect the required tunneling current of 0.04 nA (the condition of the images in figure 1) in such a relatively 'non-intruding' proximity, the measured STM image will be dominated by the O $2p_z$ components of the two oxygen atoms of the nitro group of the adsorbed molecule. Since the intensity of the weak band peaks at around −0.5 eV, it is plausible that the tip can collect the required tunneling current by accessing

[8] The first principles calculations for the adsorption structures and LDOS of the 2-nitro anthryl thiol molecules on Au(111) were carried out within the density functional theory (DFT) using a plane-wave basis set and Vanderbilt ultrasoft pseudopotentials for the atomic core regions, as implemented in the Vienna *ab initio* simulation package. The exchange correlation effects have been described within the generalized gradient approximation, with the use of the Perdew–Wang functional. The Tersoff and Hamann's formula and its extension were adopted to simulate STM images. The details of the computational studies will be published elsewhere by Fan X L and Lau W M.

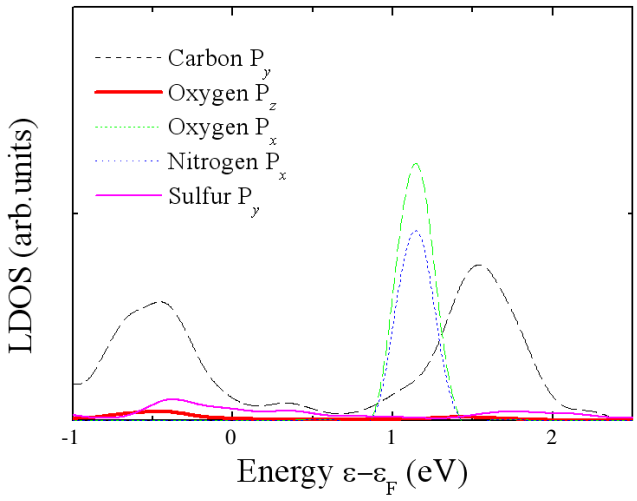

Figure 2. Projected local density of states (LDOS) onto the atomic orbital states of carbon, oxygen, nitrogen and sulfur in one molecule of the adsorbed molecules on fcc sites of Au(111).

the O $2p_z$ AO component of the band alone and without accessing the C $2p_y$ and S $2p_y$ AO components of the band. Indeed, such a simple STM image having only two 'protrusion dots' about 3 Å apart with one on the right and one on the left of the anthryl plane. The protrusion heights of the two dots are not exactly the same. As expected, tilting the molecules along the C–N axis or along the anthryl plane also affects the relative intensities of the two dots. In short, the experimental observation of two protruding-dot features about 3 Å apart at a sample–tip bias of −0.4 V is attributed to electron tunneling to the tip mainly from the O $2p_z$ AO contributions of the two oxygen atoms of the nitro group in the narrow LDOS band below the Fermi level, when the tip is approaching the nitro group from the 'vacuum'. The tip is relatively close to the oxygen atoms of the adsorbate molecule and can thus generate a relatively sharp image of the well-localized O $2p_z$ AO contributions in the narrow LDOS band below the Fermi level. On the other hand, the tip is relatively far in proximity from other atoms of the molecule. The tunneling current from the C $2p_y$ AO component of the LDOS band is weak and blurred, and there is no tunneling current from the S $2p_y$ AO component. An oblong STM protrusion background is thus generated and superimposed on the sharp protruding-dot features.

For a bias of −0.2 V, the tip collects electrons tunneling from around −0.2 eV of the narrow LDOS band below the Fermi level. The band intensity at −0.2 eV is much lower than that at −0.4 eV. It is conceivable that the tip may have to move further down and more intrusively to the molecule before it can access a high enough intensity of LDOS for the collection of the required tunneling current of 0.4 nA. Under this 'more intruding proximity', the tip probes both the O $2p_z$ and C $2p_y$ AO contributions to the LDOS band at −0.2 eV. The oblong STM protrusions can thus be more dominant than the protruding-dot features.

Under other biasing conditions, the tip may interact with LDOS having other AO contributions such as O $2p_x$ and N $2p_x$. When the bias is relatively high, the proximity separation between the tip and AO sources of the LDOS does not have to be small. The 'imaging' resolution may thus be compromised and images become blurry. The convolution of all AO sources of the relevant LDOS can thus yield a general oblong protrusion image relatively insensitive to the actual biasing condition.

Based on the above discussion, a structural model is proposed for the SAM structure of MPNAA on Au(111). The model is shown in figure 3, where it is superimposed on the STM images. The model takes into account the following considerations:

(i) The oxygen atoms of the molecules are placed near the centers of the imaged protrusions in figure 3(a). Since the two oxygen atoms in molecules M1 and M2 are imaged differently in size and brightness, one can tell that for both molecules the two oxygen atoms must be at different height levels and, in turn, that the long molecular axes of both must be tilted away from the surface normal. This is why the anthryl groups of the two are put not directly below the nitro groups, conversely, shifted away a little. As for M3 and M4, the two oxygen atoms should be nearly at the same height level.

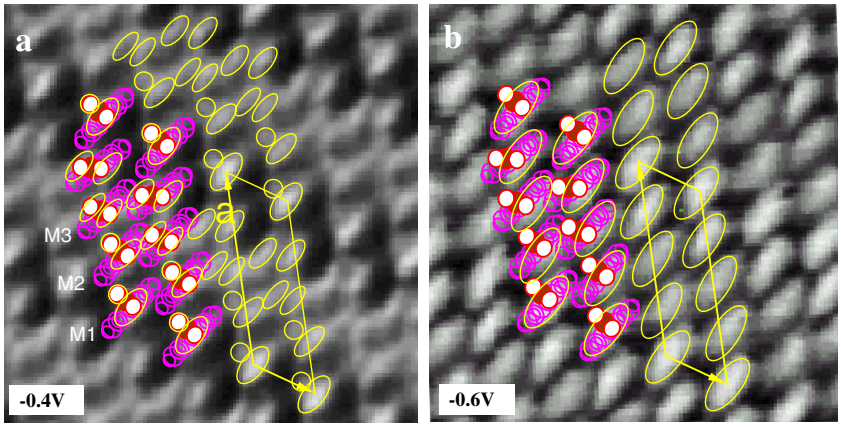

Figure 3. Zoom-in STM images (a) from figure 1(c), and (b) from figure 1(b). In both images the molecules are schematically shown according to the proposed model, with M1, M2, M3, and M4 representing the four molecules with different locations in each unit cell.

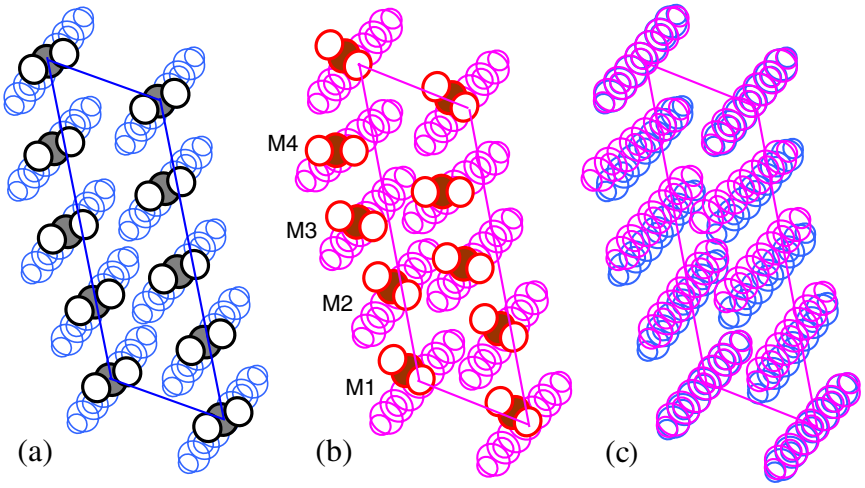

Figure 4. The models proposed (a) in [11] and (b) in the present study, as well as (c) the comparison of the two. For clarity, the nitro groups are not shown in (c).

(ii) We superimpose the molecules of M1 and M2 along with the nitro groups of M3 and M4 onto the image in figure 3(b) such that the anthryl groups of M1 and M2 just fit their corresponding oblong features. Note that for both M1 and M2 the lower oxygen atom is put outside the oblong because it makes a much smaller or even no contribution to the imaged feature.

(iii) To make M3 and M4 complete, we add the anthryl groups to their nitro groups and put them at the appropriate positions. In doing so, we have to ensure we do not violate the van der Waals (vdWs) dimensions of all molecules. It turns out that the long axes of both M3 and M4 also have to be tilted from the surface normal. However, there is a difference here: for M3 and M4 the anthryl-group planes are almost parallel to the surface normal despite the tilting, while for M1 and M2 tilting makes their anthryl-group planes rotate away from the surface normal. Thus, we designate the tilting of M1 and M2 as off-plane tilting (or OPT) and that of M3 and M4 as in-plane tilting (or IPT). Nevertheless, in the top view the tilting in both cases makes the nitro groups shift away a little with respect to their anthryl groups, as depicted in the model. To see the agreement between the model and the image in figure 3(b), one should remember that the lower portion of a molecule contributes much less to the STM tunneling current and thus make almost no contribution to the imaged feature at that bias voltage.

To compare the present model with the previous one [11], we turn to figure 4. From figure 4(c), where for simplicity only the anthryl groups are shown, we can see that the anthryl groups in the present model are actually located very close to those of their counterparts in the previous model. In other words, the molecules in the present model also form wavelike rows, which has been shown to be dominated by the parallel-displaced π–π stacking interactions and the most important common structural feature of the SAMs of the four different anthracene-based thiols [11]. However, based on the high-resolution bias-dependent STM images, we emphasize that

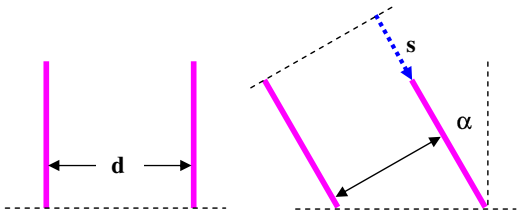

Figure 5. Schematic drawings of two parallel anthryl groups viewed along their long direction: left, without tilting; right, after introducing an off-plane tilting with an angle of α, and thus resulting in a shift (or parallel-displacement) s essentially in the short direction of the anthryl groups along with a reduced perpendicular distance $d\cos\alpha$.

the present model contains the following structural details in addition to those shown in the previous model.

(i) The long axes of all four molecules in a unit cell are tilted away from the surface normal, although OPT for M1 and M2, while IPT for M3 and M4.

(ii) For all four molecules there is a large angle between their nitro-group plane and anthryl-group plane.

As for the reason for the molecules tilting in their long axis away from the surface normal, we assume that the major driving forces behind both IPT and OPT are the π–π stacking interactions between the anthryl groups of two neighboring molecules. To clarify this, we rely on the idea of 'π-atom model' [15], in which the σ-framework and π-electrons of π-systems are considered separately. Then, one conclusion drawn is that favorable interactions are actually the π–σ attractions that overcome π–π repulsions, which prefer an offset or slipped geometry. On the basis of this idea and looking at the schematic drawings in figure 5, it is evident that an OPT can indeed enhance the π–π interactions by introducing a relative shift and reducing the perpendicular separation between the two anthryl groups.

Similarly, from the schematic drawing in figure 6 one can find that an IPT can also enhance the π–π interactions by introducing relative shifts for the parts of the two anthryl

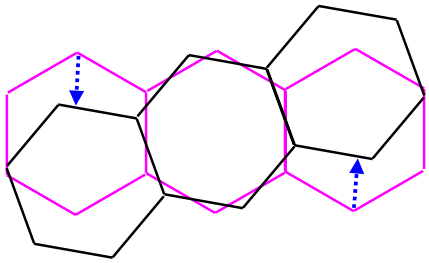

Figure 6. Schematic drawing of two anthryl groups, showing that relative rotations similar to those involved in IPTs can introduce shifts in some degree to the parts of the groups.

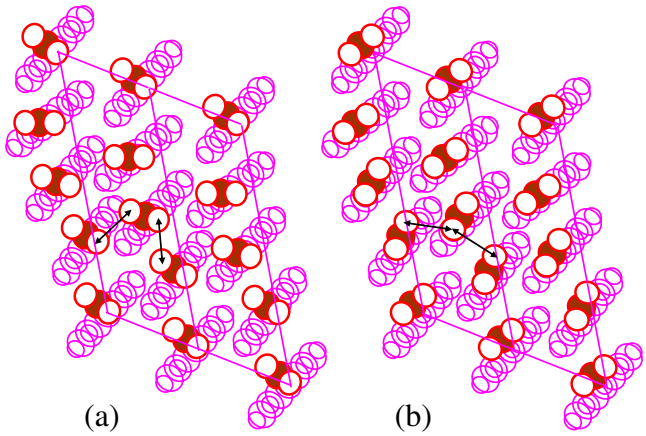

Figure 7. (a) The structural model proposed for the MPNAA SAM. (b) The same model but with the nitro groups aligned nearly coplanar with the respective anthryl groups. The double- headed arrows, showing the shortest oxygen–oxygen distances in both models, are essentially the same, and thus the large angles between the nitro and anthryl group of the molecule could not be a result of the intermolecular electrostatic interactions.

groups. Under a similar consideration, one can also find that tilting consisting of both OPT and IPT may also enhance the π–π interactions. However, the fact that both IPT and OPT may cause attractive π–π interactions between two neighboring anthryl groups is not the whole reason for inclusion of the IPTs and OPTs in the model, because in the old model shown in figure 4(a), despite having neither IPT nor OPT, attractive π–π interactions can still appear but only as a result of parallel-displacements or shifts essentially in the long direction of the anthryl groups. Actually, inclusion of both IPTs and OPTs in the present model is based on the consideration that for long π-systems of the anthryl groups, in order to introduce attractive π–π interaction shifts in the short direction of the anthryl groups are preferred.

It is not difficult to understand why this feature appears in our case, merely on the basis of the 'π-atom model' [15]. However, instead of making a detour to elaborate the argument we choose to convince the reader by citing several references. For instance, in the *ab initio* study the lowest-energy structure of a naphthalene trimer was found to be the edge-to-face geometry in which the three equivalent naphthalene moieties are arranged with their long in-plane axes parallel, on the contrary the trimer with the short in-plane axes parallel was least favorable [16]. In another recent *ab initio* study it was also concluded that for the naphthalene dimer as well as the naphthalene–anthracene complex the most favorable structure among all tested was the one with the long in-plane axes of the consisting moieties parallel [17]. More recently, the polymorphs of pentacene films were modeled, it was concluded that the herringbone structure exists in all polymorphs, that is, the long in-plane axes of the pentacene molecules are parallel [18]. It should be pointed out that although in these studies more than two molecules were involved their conclusions ought to be valid for two-body π–π cases, because for π–π interactions many-body terms are negligible [19]. In light of these considerations, we come to the conclusion that the IPTs and/or OPTs of the molecules in the MPNAA SAM are mainly the result of the intermolecular π–π interactions.

Now, we consider the driving force behind the second structural feature of a large angle between the nitro-group and anthryl-group planes for all molecules in the MPNAA SAM. The answer seems to be quite straightforward: it should be the result of the repulsive electrostatic interactions between the oxygen atoms of the nitro groups, rather than an intrinsic property of MPNAA molecules, because the strong conjugation of the nitro and anthryl groups should be able to make the former become coplanar with the latter [14]. However, this possibility can be ruled out according to the schematic drawings in figure 7. Moreover, our preliminary calculations have shown that it is an intrinsic property of MPNAA to have an angle of about 54° between its nitro and anthryl groups (see footnote 8). In other words, the large angles are a result of the intramolecular interactions (see footnote 8).

Moreover, we recall that the MPNAA SAM, compared to the SAM of the same kind of molecules but without the nitro group, has another feature, that is, the molecules in the present SAM distribute less tightly but more evenly [11]. Obviously, this special molecular packing state in the MPNAA SAM is due to the repulsive electrostatic intermolecular interactions between the negatively charged nitro groups [14], and can be understood by considering the separation dependence of such interactions.

Because the SAM structures of flexible molecules must be a balance of all involved competing interactions, including adsorbate–substrate, intermolecular, and intramolecular interactions [1–3], an important question is where the flexibilities of the present rigid molecule–substrate system come from, and how the compromises are made. For the MPNAA/Au(111) system the answers are the following.

(i) The major intermolecular interaction (π–π interactions) is very flexible itself because of its rich geometry dependence [15].
(ii) The horizontally positioned anthryl group provides more possible geometries for π–π interactions.
(iii) The adsorbate–substrate interaction is strong but essentially just induces molecules to be tethered to the substrate, because the S–Au bonding may take various adsorption sites [3, 14], may be densely populated up to one every 3

Au-atoms [1, 2, 20, 21], and may be tilted [1, 2, 14] despite its sp^3 character [21].

(iv) Inclusion of the phenyl–acetylene spacer causes the SAM to take full advantage of all these flexibilities.

(v) Finally, the electrostatic interactions among the nitro groups are, in terms of distance dependence, are also quite flexible compared to bond-formation interactions, such as H-bonding, and thus essentially impose no restrictions on the SAM structure.

Based on the above considerations, we would speculate that if the anthryl group of MPNAA is substituted by a pentacene group, similar SAMs should be able to form. Molecules in such SAMs are expected to be arranged less densely (a molecule on average is estimated to occupy a surface area of about 12 Au-atoms), and the SAMs, compared to the present ones, are expected to be even more stable against attachment of additional functional groups.

4. Summary

Careful analysis of the bias-dependent sub-molecular features in the high-resolution STM images of the MPNAA/Au(111) SAM reveals important structural details of the SAM that were missing in the previous study [11]. Specifically, (i) the long axes of the molecules are significantly tilted from the surface normal, and (ii) the nitro groups are far from being co-planar with their respective anthryl groups. We remark that tilts of the long axes of the molecules are mainly required by the intermolecular π–π interactions, while the large angles between the nitro-group and anthryl-group planes are a result of the intramolecular interactions.

The flexibility of the MPNAA/Au(111) system is discussed in detail, which is believed to originate from the following factors: (i) the major intermolecular interaction (π–π interactions) is strong but very flexible; (ii) the horizontally positioned anthryl group allows more possible geometries for π–π interactions; (iii) inclusion of the phenyl–acetylene spacer makes the SAM able to take full advantage of all these possibilities; (iv) the strong adsorbate–substrate interaction does not impose any restrictions to the SAM structure, other than tethering the molecules to the surface; and (v) different tail groups such as nitro groups, not introducing tough bond-formation interactions, are tolerable to being attached for expanding applications. Obviously, SAMs with such high flexibilities should be promising for applications in various fields.

Acknowledgments

The work in Beijing was financially supported by the National Science Foundation and Ministry of Science and Technology of China. The work in Xian was supported by the 111 Project. This work in Hong Kong was supported by two earmarked grants from the Research Grant Council of Hong Kong, with reference numbers 402803 and 401303. The work in Canada was supported by Surface Science Western and the NSERC Discovery Grant and CIAM Grant to W M Lau. The financial support from the Air Force Office of Scientific Research (AFOSR-BIC) and Army Research Office (ARO-DURINT) are also appreciated.

References

[1] Ulman A 1996 *Chem. Rev.* **96** 1533–54
[2] Schreiber F 2001 *Prog. Surf. Sci.* **65** 151–256
[3] Zharnikov M and Grunze M 2001 *J. Phys.: Condens. Matter* **13** 11333–65
[4] Yasseri A A, Syomin D, Malinovskii V L, Loewe R S, Lindsey J S, Zaera F and Bocian D F 2004 *J. Am. Chem. Soc.* **126** 11944–53
[5] Lu X, Zhang L, Li M, Wang X, Zhang Y, Liu X and Zuo G 2006 *Chem. Phys. Chem.* **7** 854–62
[6] Wei J J, Schafmeister C, Bird G, Paul A, Naaman R and Waldeck D H 2006 *J. Phys. Chem.* B **110** 1301–8
[7] Wang S, Liu Y, Huang X, Yu G and Zhu D 2003 *J. Phys. Chem.* B **107** 12639–42
[8] Krings N, Strehblow H-H, Kohnert J and Martin H-D 2003 *Electrochim. Acta* **49** 167–74
[9] Zareie M H, Ma H, Reed B W, Jen A K-Y and Sarikaya M 2003 *Nano Lett.* **3** 139–42
[10] Kang S H, Ma H, Kang M S, Kim K-S, Jen A K-Y, Zareie M H and Sarikaya M 2004 *Angew. Chem. Int. Edn* **43** 1512–6
[11] Dou R F, Ma X C, Xi L, Yip H L, Wong K Y, Lau W M, Jia J F, Xue Q K, Yang W S, Ma H and Jen A K Y 2006 *Langmuir* **22** 3049–56
[12] Saenger W 1984 *Principles of Nucleic Acid Structure* (New York: Springer) pp 261–5
[13] McGaughey G B, Gagné M and Rappé A K 1998 *J. Biol. Chem.* **273** 15458–63
[14] Ulman A 2001 *Acc. Chem. Res.* **34** 855–63
Kang J F, Ulman A, Liao S and Jordan R 1999 *Langmuir* **15** 2095–8
Kang J F, Ulman A, Liao S, Jordan R, Yang G H and Liu G Y 2001 *Langmuir* **17** 95–106
[15] Hunter C A and Sanders J K M 1990 *J. Am. Chem. Soc.* **112** 5525–34
[16] Gonzalez C and Lim E C 1999 *J. Phys. Chem.* A **103** 1437–41
[17] Lee N K, Park S and Kim S K 2000 *J. Chem. Phys.* **116** 7910–7
[18] Mattheus C C, de Wijs G A, de Groot R A and Palstra T T M 2003 *J. Am. Chem. Soc.* **125** 6323–30
[19] Tauer T P and Sherrill C D 2005 *J. Phys. Chem.* A **109** 10475–8
[20] Wan L J, Terashima M, Noda H and Osawa M 2000 *J. Phys. Chem.* B **104** 3563–9
[21] Cyganik P and Buck M 2004 *J. Am. Chem. Soc.* **126** 5960–1